JOURNAL OF Applied Polymer SCIENCE

Hydrolysis and Thermal Degradation of Poly(L-Lactide) in the Presence of Talc and Modified Talc

Mi-Yeong Jo, Yeon Jong Ryu, Jun Hee Ko, Jin-San Yoon
Department of Polymer Science and Engineering, Inha University, Yonghyun-dong, Nam-gu, Incheon 402-751, Korea
Correspondence to: J.-S. Yoon (E-mail: jsyoon@inha.ac.kr)

ABSTRACT: Talc and talc modified with trimethoxy(octadecyl)silane (O-talc) were melt compounded with poly (L-lactide) (PLA). The crystallization behavior, tensile properties, and impact strength of the PLA composites were examined before and after the incorporation of talc and O-talc. The molecular weight of PLA in the PLA composites was measured as a function of the hydrolysis time and temperature. The effect of talc and O-talc on the thermal stability of PLA was examined and quantified by the activation energy of thermal degradation and the integral procedural decomposition temperature value determined from the corresponding thermo-gravimetric analysis weight loss profiles. © 2012 Wiley Periodicals, Inc. J. Appl. Polym. Sci. 129: 1019–1025, 2013

KEYWORDS: biomaterials; composites; thermal properties

Received 30 August 2012; accepted 22 October 2012; published online 22 November 2012
DOI: 10.1002/app.38753

INTRODUCTION

Recently, there has been increasing interest in the development of biomass-based plastics to alleviate global warming and other environmental burden. Considerable efforts have been made to substitute fossil resource-based materials with materials from natural and crop resources.[1–6]

Poly (L-lactide) (PLA) is a biodegradable polymer that can be derived from renewable resources, such as corn and sugarcane. PLA is transparent with comparable melting point, tensile strength, and flexural strength to those of polypropylene. In addition, control of the mechanical properties of PLA is relatively easy through copolymerization or blending with other polymers and plasticizers.[7–12] PLA is applied not only for packaging but also for durable materials.[13] However, PLA has low heat stability that limits its application window.[14,15] Moreover, PLA is hydrolyzed easily in the presence of water, particularly at high temperatures.

The incorporation of talc as a filler to thermoplastics is a common practice in the plastics industries because talc makes it possible to reduce the production cost of molded products and improve the balance between toughness, stiffness, and strength.[16]

Talc acts as a nucleating agent in PLA, increases the number of spherulites and reduces the spherulite size during processing.[17–19] Battegazzire et al.[20] provided excellent information on the crystallization kinetics of PLA/talc composites. The dispersion and wettability between the matrix and the filler are essential for PLA composites with advanced material properties.[21]

In this study, the surface polarity of talc was modified by a reaction with trimethoxy(octadecyl)silane (TMOS) to improve the dispersion and wettability between PLA and talc, because PLA is less polar than talc. The concomitant change in stability against hydrolysis and thermal degradation was examined. The crystallization and mechanical properties of PLA and PLA/talc composites were also explored.

EXPERIMENTAL

Materials

PLA was purchased from NatureWorks (2003D, Minnetonka, MN). Talc (whiteness 95 min, particle size 5.5 ± 0.5 μm, bulk density 0.25 ± 0.05 g/cm^3, moisture (ppm) 3000 max, pH 8.8 ± 0.5, Kochone (KCM-6300), Suwon, Korea) was used as received. TMOS was purchased from Aldrich (St. Louis, MO).

Modification of Talc

Neat talc was dried in a convection oven at 60°C for 24 h to remove the moisture from the material before processing. A three-neck flask was predried using a heat gun and N_2. If talc and anhydrous toluene are added stepwise, the talc powder flew in all directions to make it difficult to expect the precise amount of talc. Therefore, a small amount of anhydrous toluene (10 mL) was first added in the prepared flask, and 40 g of talc was then added. The remaining anhydrous toluene (490 mL) and TMOS (4 g) was added. The solution was stirred at 110°C for 12 h under a N_2 atmosphere. The solution was then filtered, and the filtrate was washed several times with ethanol and dried in a vacuum oven at 60°C for 24 h.

Table I. Contents of the PLA/Talc Composites

Sample	PLA (wt %)	Talc (wt %)	TMOS-modified talc (wt %)
PLA	100	0	0
PLA/talc-2	98	2	0
PLA/talc-5	95	5	0
PLA/O-talc-2	98	0	2
PLA/O-talc-5	95	0	5

Preparation of PLA/Talc Composites

PLA and talc were dried in a vacuum oven at 60°C for 24 h. Composites of PLA/talc were prepared by melt compounding at 190°C using a twin screw extruder (screw diameter = 19 mm, L/D = 40, BauTechnology, Uijeongbu, Korea). Table I lists the contents of the composites. The extruded products were dried in a vacuum oven at 60°C for 24 h.

The dried products were molded at 190°C using an injection molder (screw diameter = 22 mm, clamping force = 50t, VDC-II, JinHwaGloTech, Cheonan, Korea) to prepare the test specimens.

Characterization

Mechanical Properties. The tensile properties of the composites were measured using a universal testing machine (UTM, Housefield, H10KS-0061, Surrey, England). The specimens were prepared according to ASTM D638. The cross-head speed was 50 mm/min. The notched Izod impact strength was measured using an Izod impact tester (Qmesys, QM700A, Gwangmyeong, Korea) according to ASTM D256 at room temperature. The results of at least five measurements were averaged.

Gel Permeation Chromatography (GPC). The extruded PLA, PLA/talc, and PLA/O-talc pellets, 2 mmΦ × 3 mmL in size, were subjected to hydrolysis in water at 50°C and 70°C. The pellets were withdrawn at each interval and dissolved in tetrahydrofuran (THF) after drying. The molecular weight of the pellets was measured by GPC (Pump: Waters 1515, detector: Waters 2414, Milford, MA) after filtering the solution through a 0.5-μm syringe filter. THF (at a flow rate of 1 mL/min) was used as the eluent. Polystyrene (Shodex Standard SM-105 Lot No. 60502, Tokyo, Japan) was used for calibration.

Thermal Properties. The thermal stability of PLA, PLA/talc, and PLA/O-talc was measured by thermo-gravimetric analysis (TGA, TA instruments, TGA-Q50, New Castle, DE). The sample weight was 10–15 mg and scanned to 800°C under a nitrogen atmosphere at 5, 10, 20, and 40°C/min.

The crystallization temperature of the PLA, PLA/talc, and PLA/O-talc composites was measured by differential scanning calorimetry (DSC, Perkin Elmer, DSC-7, Waltham, MA). The sample weight was 5–10 mg. The sample was heated to 220°C at a heating rate of 50°C/min to determine the first scan cold crystallization temperature and then quenched at a rate of −100°C/min to room temperature. It was reheated at 20°C/min to 220°C to obtain the second scan crystallization profiles.

Fourier Transform Infrared (FTIR). The surface modification of talc was monitored by FTIR vacuum spectrometry (FTIR, Bruker, VERTEX 80V, Billerica, MA).

Turbiscan. Turbiscan (Turbiscan^{TM}LAB, Formulation, Toulouse, France) was used to examine the dispersion stability of raw and modified talc in chloroform. The sedimentation behavior of the raw and modified talc powder in the chloroform suspension was monitored by measuring the backscattering and transmission of monochromatic light (λ = 880 nm). The suspensions in flat-bottomed cylindrical glass tubes (30 cm^3) were placed in the instrument and the transmission of light from the suspensions was then measured periodically along the height at room temperature. The sedimentation rate was evaluated from the change in backscattering intensity at the top portion of the sample.

Elemental Analyses. The contents of C and H in the talc and O- talc were identified through an element analyzer (EA, Thermo Electron Corporation, FlashEA1112, Waltham, MA). The talc and O- talc sample of 1.5–2 mg was oxidized at 900°C in an excess of oxygen (at a flow rate of 250 mL/min) with the copper oxide wires catalyst. Helium was used as a carrier gas. The mass fractions of the combustion products (carbon dioxide, water, nitrogen dioxide, sulfur dioxide) were calculated using the BBOT standard (C: 72.53%, H: 6.09%, N: 6.51%, S: 7.44%, O: 7.43%).

RESULTS AND DISCUSSION

The organo-modification of talc was attempted using TMOS to increase the wettability between the filler and the PLA matrix. Figure 1 presents the FTIR spectra of talc before and after modification. The FTIR peak corresponding to —OH stretching appearing at 3400 cm^{-1} became less intense as talc was treated with TMOS due to the exhaustion of OH groups on the talc surface by the reaction with TMOS. Table II summarizes the results of elemental analyses on the hydrogen and carbon content in talc and the modified-talc (O-talc). The gas evolving from the talc and O-talc samples after oxidation at 900°C was analyzed. The percentage of the elements was calculated based

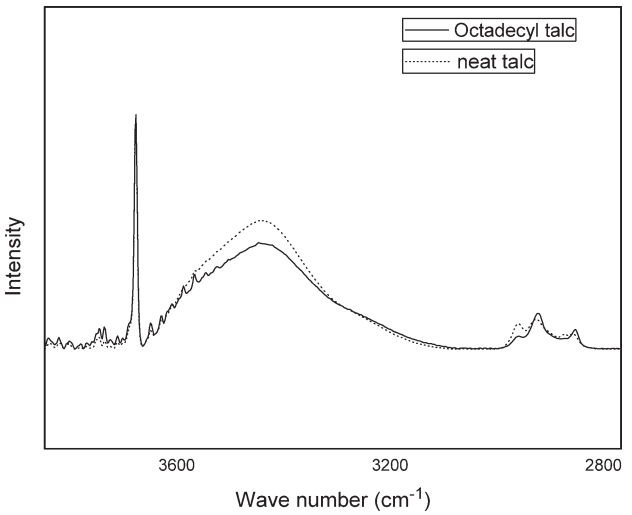

Figure 1. FTIR spectra of talc and O-talc.

Table II. Results of Elemental Analysis

Elements	Carbon	Hydrogen
Talc	1.62 wt %	0.37 wt %
Modified talc	2.06 wt %	0.54 wt %

on the weight of the initial weight of the samples. It can be seen that the hydrogen and carbon content of O-talc was higher than those of neat talc.

Figure 2 shows the stability of talc and O-talc particles suspended in chloroform measured using Turbiscan^{TM}LAB. The sedimentation velocity of O-talc in the chloroform suspension was slower than that of talc, exhibiting that the hydrophobicity of talc was increased by modification with TMOS. However, the difference in the sedimentation velocity of O-talc from that of talc is not remarkable indicating that the amount of TMOS grafted to talc was quite limited. This is because talc has a chemical formula of $Mg_3Si_4O_{10}(OH)_2$ and has very small number of —OH groups reactive toward TMOS.

PLA was melt-compounded with talc and O-talc using a co-rotating twin screw extruder. Figure 3 shows the DSC thermo-grams of the extruded PLA, PLA/Talc, and PLA/O-Talc pellets measured by DSC. The first scan DSC thermo-grams were obtained by heating the samples from room temperature to 220°C at 50°C/min, whereas the second DSC thermo-grams were obtained by reheating the samples at 20°C/min after quenching the samples at −100°C/min from 220°C to room temperature.

The second scan cold crystallization peak temperature of neat PLA appeared at 127°C, whereas that of PLA/talc-2 and PLA/talc-5 was observed at 118°C and 114°C, respectively, revealing that crystallization was accelerated in the presence of talc.[20,22–24] The effectiveness of O-talc on the crystallization of PLA was similar to that of talc, in that the cold crystallization peak of PLA/O-talc was observed at a similar temperature to that of PLA/talc.

As shown in Table III, the pellets of PLA, PLA/talc-5, and PLA/O-talc-5, as extruded from the twin screw extruder, exhibited

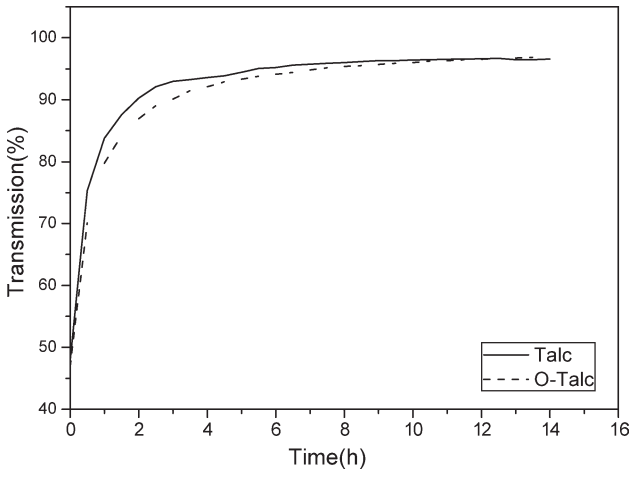

Figure 2. Turbiscan^{TM}LAB transmittance profile and settling time of talc and O-talc.

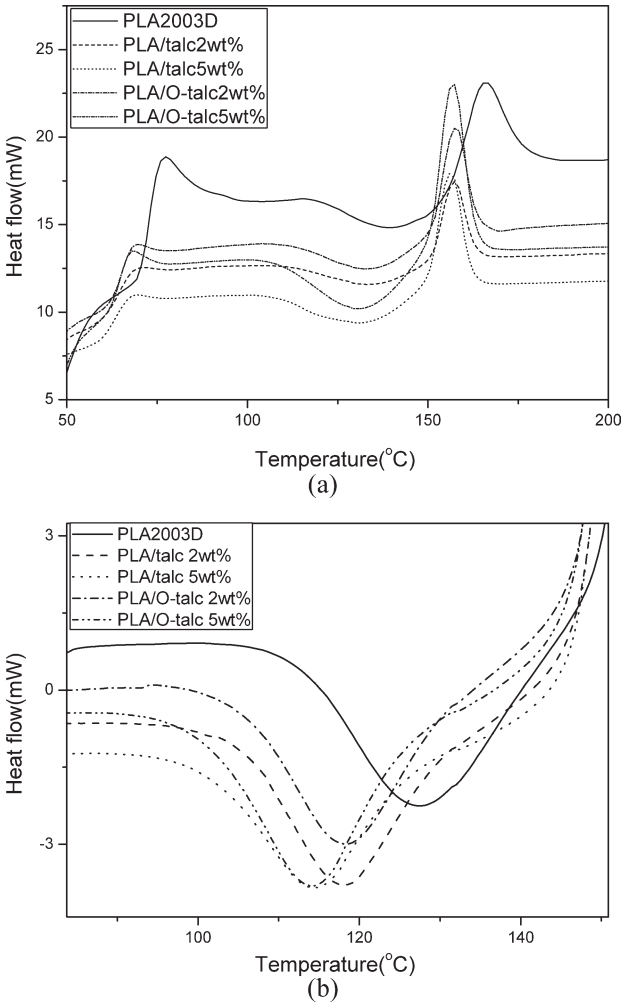

Figure 3. (a) First-scan and (b) second-scan DSC curves of PLA/talc composites as a function of the talc and modified talc content.

0.6%, 0.8%, and 0.9% of crystallinity, respectively, which was determined from the respective first scan heat of fusion and crystallization, ΔH_f and ΔH_c, respectively, based on eq. (1), assuming the heat of fusion of the perfect crystal of PLA, ΔH^0, is 93.2 J/g.[25,26]

$$\text{Crystallinity} = \frac{(\Delta H_f + \Delta H_c)}{\Delta H^0} \quad (1)$$

The as extruded PLA/talc and PLA/O-talc pellets of 2 mmΦ × 3 mmL in size were subjected to hydrolysis in water at 50°C and 70°C. Table IV lists the weight average molecular weight (Mw) of PLA measured by GPC, as a function of the hydrolysis time. At 50°C, the Mw of PLA was reduced from 164,000 to 121,000 after 10 days hydrolysis. The decrease in Mw was less pronounced in the order of PLA > PLA/talc > PLA/O-talc. However, the difference was not significant. In contrast, the Mw of PLA deceased much faster as the hydrolysis temperature was raised, in that the Mw of PLA decreased from 164,000 to 2300 after 10 days of hydrolysis at 70°C. The decrease rate of Mw of PLA was slower in the order of PLA > PLA/talc > PLA/O-talc, as was the case of the hydrolysis at 50°C. Although talc has a

Applied Polymer SCIENCE

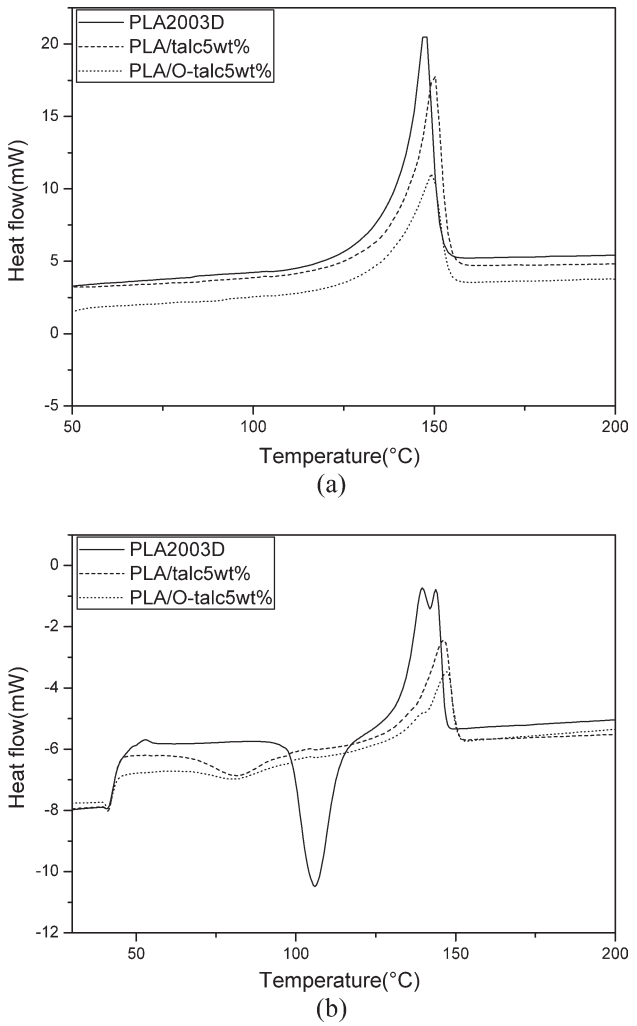

Figure 4. (a) First-scan and (b) second-scan DSC curves of PLA/talc composites as a function of the talc and modified talc content after hydrolysis.

platelet structure,[27] talc and O-talc do not increase much the tortuous path for water molecules through the composites as much as clays do, because intercalation or exfoliation of the silicate layers of talc is enormously difficult to achieve. Therefore, the reduced hydrolysis rate of PLA/talc and PLA/O-talc compared with that of neat PLA cannot be attributed to the prolonged diffusion path of water molecules. The higher crystallinity of PLA in PLA/talc and PLA/O-talc, though slightly, compared with that of neat PLA seems to be at least partly responsible for the somewhat slower initial hydrolysis rate. According to Figure 4 and Table III, the crystallinity of PLA, PLA/talc, and PLA/O-talc determined from the heat of fusion of the respective first scan DSC thermograms increased significantly after hydrolysis. This can be due to the preferential hydrolysis of the amorphous fraction of PLA and to the *in situ* unceasing crystallization of the not yet completely hydrolyzed PLA molecules during the long hydrolysis procedure. At the later stage, the difference in the crystallinity between the three kinds of pellets became similar to each other within experimental error, and thereby the hydrolysis rate of the composites did not differ from that of neat PLA any further, so that the Mw of PLA in PLA/talc and PLA/O-talc was similar to that of neat PLA after 10 days of hydrolysis at 70°C.

Table III. Crystallinity of PLA, PLA/Talc, and PLA/O-Talc before and after Hydrolysis at 70°C for 10 days

		Degree of crystallinity (%)	
Composites		First scan	Second scan
Before the hydrolysis	PLA	0.6	1.2
	PLA/talc-5	0.8	2.5
	PLA/O-talc-5	0.9	2.9
After the hydrolysis	PLA	53.2	6.1
	PLA/talc-5	52.5	20.6
	PLA/O-talc-5	52.0	29.8

The number after the sample code is the content of talc and O-talc in wt %. For example, PLA/talc-2 is the PLA composite with 2 wt % talc.

The Mw of PLA, PLA/talc, and PLA/O-talc was as low as ~ 3000 after hydrolysis at 70°C for 10 days despite their crystallinity reaching ~ 50%. This means that not only the amorphous fraction but also many of the chains tying the PLA chains in the PLA crystal lamellae were hydrolyzed off leaving short molecules behind in the PLA crystal lamellae. The similar crystallinity of PLA, PLA/talc, and PLA/O-talc after 10 days of hydrolysis

Table IV. Weight Average Molecular Weight of PLA, PLA/Talc, and PLA/O-Talc as a Function of the Hydrolysis Time

Temperature	Hydrolysis time	PLA	PLA/talc-2	PLA/talc-5	PLA/O-talc-2	PLA/O-talc-5
50°C	0 days	164,000	186,000	191,000	189,000	193,000
	1 day	158,000	182,000	188,000	185,000	192,000
	3 days	140,000	175,000	181,000	178,000	185,000
	5 days	134,000	165,000	173,000	169,000	178,000
	10 days	121,000	156,000	161,000	158,000	167,000
70°C	0 days	164,000	186,000	191,000	189,000	193,000
	1 day	90,000	95,000	108,000	96,000	121,000
	3 days	19,500	31,300	37,000	34,400	43,900
	5 days	5400	8500	14,600	14,900	19,000
	10 days	2300	2800	3000	2900	3200

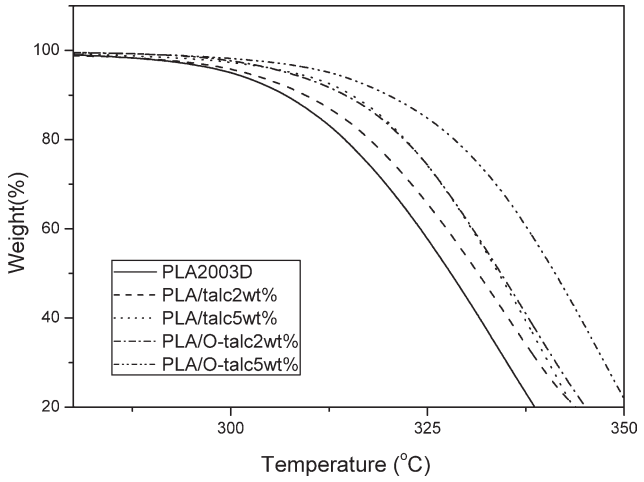

Figure 5. TGA profiles of PLA, PLA/talc, and PLA/O-talc composites.

supports this hypothesis. It is interesting to observe that, at the initial stage, the crystallinity of PLA determined from the second DSC scan was not much lower than that of PLA/talc and PLA/O-talc, whereas, at the final stage, the second DSC scan resulted in significantly higher crystallinity of PLA/talc and PLA/O-talc compared with that of neat PLA. The lower the molecular weight of PLA, the faster the crystallization, and thereby the more affected was the crystallization by talc and O-talc.

Interestingly, the initial Mw of neat PLA was lower than that of PLA in PLA/talc and PLA/O-talc. As neat PLA was extruded under the same conditions as PLA/talc and PLA/O-talc, the higher initial Mw of PLA in PLA/talc and PLA/O-talc compared with that of neat PLA suggests that talc and O-talc can be effective in repressing the thermal degradation of PLA during the melt compounding.

Figure 5 displays the thermal degradation behavior of PLA, PLA/talc, and PLA/O-talc observed by TGA. The onset temperature of weight loss increased in the order of PLA < PLA/talc-2 < PLA/talc-5 ≒ PLA/O-talc-2 < PLA/O-talc-5, as summarized in Table V, indicating that talc and O-talc contributed to the thermal stabilization of PLA. Here, $T_{10\%}$, $T_{20\%}$, and $T_{30\%}$ represent the temperatures corresponding to 10%, 20%, and 30% of weight loss, respectively. Because the thermal degradation of PLA should not depend on the crystallinity as much as hydrolysis, the enhanced thermal stability as a result of incorporation of talc and O-talc is not due to the increased crystallinity but to the thermal stabilization effect of the solid filler in a similar manner to clay in many other polymers.[28–31]

Table V. Temperatures Corresponding to 10%, 20%, and 30% of Weight Loss for PLA, PLA/Talc, and PLA/O-Talc Composites

Samples	PLA	PLA/ talc-2	PLA/ talc-5	PLA/ O-talc-2	PLA/ O-talc-5
$T_{10\%}$	306	309	315.0	314	320
$T_{20\%}$	314	317	322	322	328
$T_{30\%}$	320	323	327	327	334

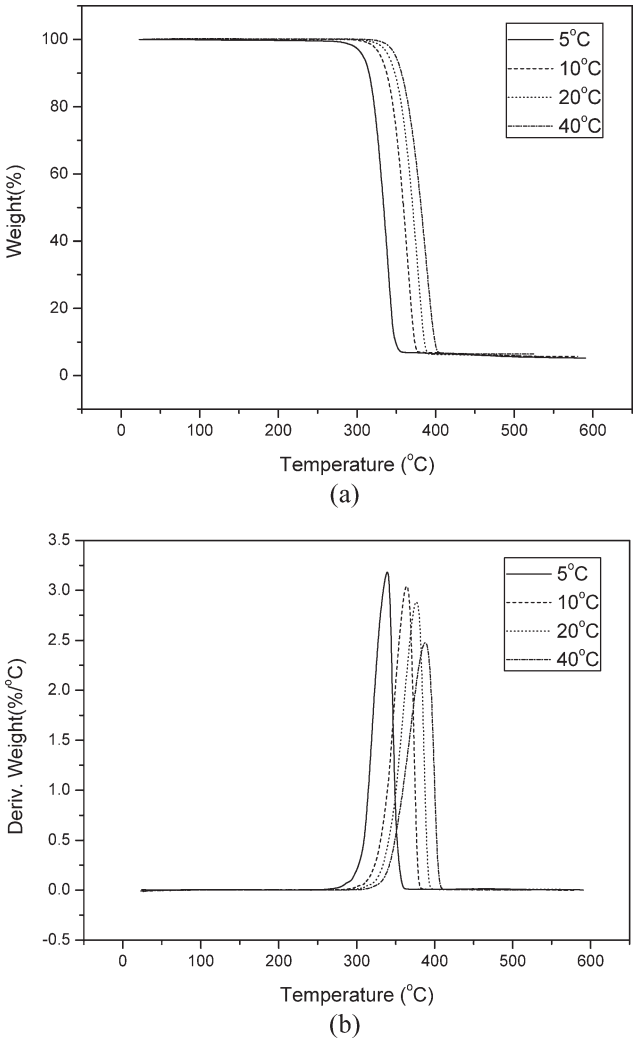

Figure 6. TGA curves of PLA, PLA/talc, and PLA/O-talc at different heating rates (5, 10, 20, and 40°C/min) (a) and corresponding DTA curves (b).

To quantify the thermal stabilization effect of talc and O-talc, the activation energy of the thermal degradation of PLA, PLA/talc, and PLA/O-talc was determined experimentally from the corresponding TGA thermal degradation profiles, and the values were compared with each other. According to the Kissinger's equation, as expressed in eq. (2), the activation energy of thermal degradation, E, can be determined from the slope of the linear relationship between $\ln(\beta/T_{max}^2)$ and $1/T_{max}$:

$$\ln\frac{\beta}{T_{max}^2} = \left\{\ln\frac{AR}{E} + \ln[n(1-\alpha_{max})^{n-1}]\right\} - \frac{E}{RT_{max}} \qquad (2)$$

where T_{max} is the temperature corresponding to the maximum in the thermal degradation rate profiles at different scanning rates, β, as shown in Figure 6.[32]

Figure 7 presents a plot of the linear relationship of the Kissinger's equation and the activation energy of thermal degradation was obtained from the slope in Figure 7. The activation energy of thermal degradation of neat PLA was 116 ± 0.2 kJ/mol,

Applied Polymer SCIENCE

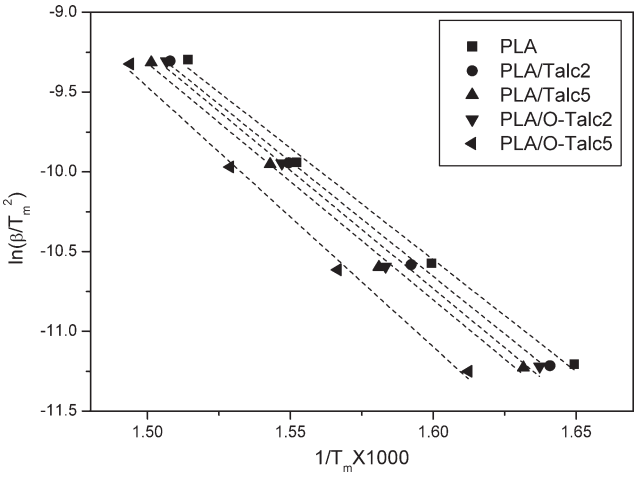

Figure 7. Plots for the determination of the activation energies of thermal degradation for PLA, PLA/talc, and PLA/O-talc according to the Kissinger's equation.

whereas those of PLA/talc-2 and PLA/talc-5 were 119 ± 0.5 and 123 ± 0.2 kJ/mol, respectively. In case of PLA/O-talc-2 and PLA/O-talc-5, the corresponding values were 123 ± 0.2 and 135 ± 0.1 kJ/mol, respectively, confirming the positive effect of talc and O-talc on the thermal stabilization of PLA.

The integral procedural decomposition temperature (IPDT) is another index to assess the thermal stabilization, as expressed in eq. (3) and Figure 8.[33]

$$\mathrm{IPDT}(^{\circ}\mathrm{C}) = \mathrm{A} \cdot \mathrm{K} \cdot (\mathrm{T_f} - \mathrm{T_i}) + \mathrm{T_i} \quad (3)$$

Table VI shows that the IPDT value increased in the order of PLA < PLA/talc-2 < PLA/O-talc-2 < PLA/talc-5 < PLA/O-talc-5. The order was slightly different from that of the activation energy of thermal degradation. However, the more positive effect of O-talc on the thermal stabilization of PLA than that of talc can be confirmed again.

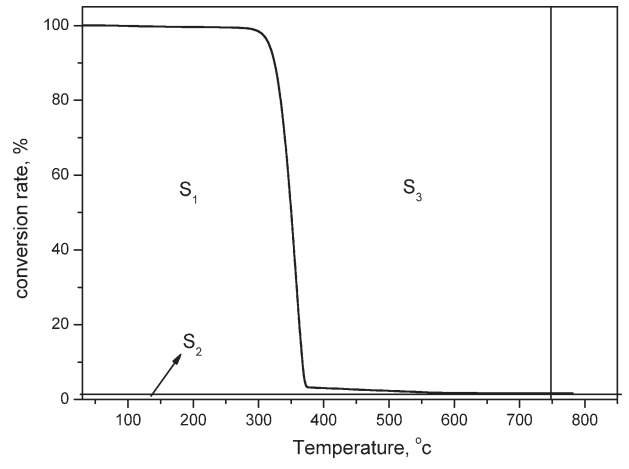

Figure 8. Schematic diagram of S_1, S_2, and S_3 for the calculation of A and K.

Table VI. IPDT Values of PLA, PLA/Talc, and PLA/O-Talc

Composites	PLA	PLA/ talc-2	PLA/ talc-5	PLA/ O-talc-2	PLA/ O-talc-5
A^a	0.571	0.573	0.586	0.581	0.590
K^b	1.025	1.051	1.089	1.053	1.091
IPDT (°C)	341 ± 0.2	350 ± 0.5	369 ± 0.1	355 ± 0.1	372 ± 0.4

$A^a = (S_1 + S_2)/(S_1 + S_2 + S_3)$, $K^b = (S_1 + S_2)/S_1$.

Table VII lists the mechanical properties of the resulting PLA/talc and PLA/O-talc composites. The tensile strength of PLA was reduced from 706 to 678 and 663 kgf/cm^2, respectively, as a result of the incorporation of 2 and 5 wt % talc, respectively, despite the positive effect of talc on the crystallization of PLA in PLA/talc. This can be rationalized by the fact that interfacial interaction between PLA and talc was not strong enough to withstand the tensile force. The higher tensile strengths of PLA/O-talc-2 and PLA/O-talc-5 compared with those of PLA/talc-2 and PLA/talc-5, respectively, were attributed to the enhancement of interfacial interaction by treating talc with TMOS. The tensile strain varied in the same manner as the tensile strength, in that it was 10.4% for the neat PLA, whereas PLA/talc and PLA/O-talc manifested 6.7 and 7.8% of the tensile strain, respectively.

Interestingly, the impact strength of the neat PLA was 2.89 kgf cm/cm, whereas PLA/talc-2 and PLA/talc-5 exhibited 3.07 and 3.23 kgf cm/cm of impact strength, respectively, despite the decreased tensile strength and strain of the composites. This may be attributed to the smaller spherulites of PLA in PLA/talc than those in the neat PLA.

The dependence of the impact strength on the spherulite size has been reported for many other polymers.[34,35] The slightly higher impact strength of PLA/O-talc compared with PLA/talc was attributed to the reduced spherulite size due to the more effective nucleation of O-talc compared with talc as well as from the more favorable interfacial interaction between PLA and O-talc rather than talc.

Direct measurements of the spherulite size of the PLA in the specimens for the mechanical tests were unsuccessful. Further study will be needed to observe spherulite growth during extrusion and injection molding and to clarify the relationship between the impact strength and spherulite size of PLA.

Table VII. Mechanical Properties of PLA, PLA/Talc, and PLA/O-Talc

Items	PLA	PLA/ talc-2	PLA/ talc-5	PLA/ O-talc-2	PLA/ O-talc-5
Tensile strength (kgf/cm^2)	711	678	663	694	683
Impact strength (kgf cm/cm)	2.89	3.07	3.23	3.33	3.41
Elongation at break (%)	10.4	7.05	6.72	7.22	7.76

CONCLUSIONS

Talc was modified with TMOS to prepare O-talc. The initial hydrolysis rate of PLA/talc and PLA/O-talc pellets was somewhat slower than that of the neat PLA, which is in line with the order of increased crystallinity of PLA in the composites. The crystallinity of PLA, PLA/talc, and PLA/O-talc was increased after hydrolysis due to the preferential hydrolysis of the amorphous fraction of PLA and to the *in situ* unceasing crystallization of the not yet completely hydrolyzed PLA molecules during hydrolysis. The Mw of PLA, PLA/talc, and PLA/O-talc decreased to as low as $\sim$ 3000 after hydrolysis at 70°C for 10 days despite their crystallinity reaching $\sim$ 50%, indicating that not only the PLA molecules outside the PLA crystals but also many of the PLA chains tying the chains inside the PLA crystal lamellae were hydrolyzed off leaving short molecules behind in the PLA crystal lamellae. Talc and O-talc contributed to the thermal stabilization of PLA, which is supported by the activation energy of thermal degradation determined from the TGA profile using the Kissinger's equation and the IPDT value. The incorporation of talc into PLA reduced the tensile strength and strain but enhanced the impact strength. The decrease in tensile strength and strain was less pronounced, and the improvement in impact strength was more significant when O-talc was incorporated instead of talc. This was rationalized by the improved interfacial interaction between the components and the reduced size of the spherulites of PLA in PLA/O-talc than that in PLA/talc.

ACKNOWLEDGMENTS

This study was supported by the National Research Foundation of Korea (NRF), contact grant number: 2010-0010822.

REFERENCES

1. Rout, J.; Misra, M.; Tripathy, S. S.; Nayak, S. K.; Mohanty, A. K. *Polym. Compos.* **2001**, *22*, 770.
2. Mohanty, A. K.; Drzal, L. T.; Hokens, D.; Misra, M. *Polym. Mater. Sci. Eng.* **2001**, *85*, 594.
3. Tripathy, S. S.; Levita, G.; Landro, D. *Polym. Compos.* **2001**, *22*, 815.
4. Song, Y. P.; Wang, D. Y.; Wang, X. L.; Lin, L.; Wang, Y. Z. *Polym. Adv. Technol.* **2011**, *22*, 2295.
5. Kontou, E.; Niaounakis, M.; Georgiopoulos, P. *J. Appl. Polym. Sci.* **2011**, *122*, 1519.
6. Tang, Z.; Zhang, C.; Liu, X.; Zhu, J. *J. Appl. Polym. Sci.* **2012**, *125*, 1108.
7. Yokohara, T.; Yamaguchi, M. *Eur. Polym. J.* **2008**, *44*, 677.
8. Kang, K. S.; Shin, B. Y. *Korean Chem. Eng. Res.* **2007**, *46*, 124.
9. Ke, T.; Sun, S. *Cereal Chem.* **2000**, *77*, 761.
10. Jacobson, S.; Fritz, H. G. *Polym. Eng. Sci.* **1996**, *36*, 2799.
11. Ogata, N.; Jimenez, G.; Kawai, H.; Ogihara, T. *J. Polym. Sci. Part B: Polym. Phys.* **1997**, *35*, 389.
12. Zhang, L.; Goh, S. H.; Lee, S. Y. *Polymer* **1998**, *39*, 4841.
13. David, S. B.; Geyer, J. D.; Gustafson, A.; Snook, J.; Narayan, R. In Biodegradable Plastics and Polymers; Doi, Y., Fukuda, K., Eds.; Elsevier: Osaka, **1993**; p 601.
14. Jang, M. O.; Nam, B. U.; Jeong, D. S.; Hong, C. H. *Appl. Chem.* **2010**, *14*, 1.
15. Lee, B. I.; Kim, S. H.; Lee, M. S. *Text. Sci. Eng.* **2008**, *45*, 269.
16. Shi, Q. F.; Mou, H. Y.; Li, Q. Y.; Wang, J. K.; Guo, W. H. *J. Appl. Polym. Sci.* **2012**, *123*, 2828.
17. Thakur, K. A. M.; Kean, R. T.; Zupfer, J. M.; Buehler, N. U.; Doscotch, M.; Munson, E. *Macromolecules* **1996**, *29*, 8844.
18. Hiljanen-Vainio, M.; Heino, M.; Seppälä, J. V. *Polymer* **1998**, *39*, 865.
19. Huda, M.; Drzal, L.; Misra, M. *Ind. Eng. Chem. Res.* **2005**, *44*, 5593.
20. Battegazzire, D.; Bocchini, S.; Frache, A. *eXPRESS Polym. Lett.* **2011**, *5*, 849.
21. Fowlks, A. C.; Narayan, R. *J. Appl. Polym. Sci.* **2010**, *118*, 2810.
22. Papageorgiou, G. Z.; Achilias, D. S.; Bikiaris, D. N.; Karayannidis, G. P. *Thermochim. Acta* **2005**, *427*, 117.
23. Radhakrishnan, S.; Sonawane, P. S. *J. Appl. Polym. Sci.* **2003**, *89*, 2994.
24. Radhakrishnan, S.; Sonawane, P. S.; Pawaskar, N. *J. Appl. Polym. Sci.* **2004**, *93*, 615.
25. Fisher, E. W.; Sterzel, H. J.; Wegner, G. *Colloid Polym. Sci.* **1973**, *251*, 980.
26. Buzarovska, A.; Grozdanov, A. *J. Appl. Polym. Sci.* **2012**, *123*, 2187.
27. Yu, F.; Liu, T.; Zhao, X.; Yu, X.; Lu, A.; Wang, J. *J. Appl. Polym. Sci.* **2012**, *125*, E99.
28. Paul, M. A.; Alexandre, M.; Degee, P.; Henrist, C.; Rulmont, A.; Dubois, P. *Polymer* **2003**, *44*, 443.
29. Chang, J. H.; An, Y. U.; Sur, G. S. *J. Polym. Sci.* **2003**, *41*, 94.
30. Wu, D.; Wu, L.; Wu, L.; Zhang, M. *Polym. Degrad. Stab.* **2006**, *91*, 3149.
31. Lim, S. T.; Hyun, Y. H.; Choi, H. J.; Jhon, M. S. *Chem. Mater.* **2002**, *14*, 1839.
32. Kissiger, H. E. *Anal. Chem.* **1957**, *29*, 1702.
33. Doyle, C. D. *Anal. Chem.* **1961**, *33*, 77.
34. Svoboda, P.; Zeng, C.; Wang, H.; Lee, L. J.; Tomasko, D. L. *J. Appl. Polym. Sci.* **2002**, *85*, 1562.
35. Perkins, W. G. *Polym. Eng. Sci.* **1999**, *39*, 2445.